RF Front End Module Architectures for 5G

Florinel Balteanu

Skyworks Solutions Inc., CA92617, USA

florinel.balteanu@skyworksinc.com

***Abstract*— Worldwide adoption of 3G/4G smartphones for more than 5 billion of people has been one of the main driving engine behind semiconductor industry. 5G is expected to bring higher data capacity, low latency and new RF hardware enhancements which will open the market for new application where our smartphones will be a conduit. CMOS lower features nodes as FinFET 7nm/14nm CMOS allow the computational power and lower power consumption required for the use of digital signal processing and RF digital calibration which are essential for 4G/5G modem and application processor technology. The goal of having a single die for the entire 4G/5G functionality has faded away to a more realistic partitioning where many RF and analogue blocks are integrated with other components such as RF acoustic filters in multiple RF front-end-modules. This paper presents RF front end architectures which will be part of 5G smartphones together with circuit and measurement details.**

Keywords—RF front end (RFFE), front end module (FEM), switch, power management IC (PMIC), GSM, 3G, 4G, 5G, GPS, long term evolution (LTE), new radio (NR), user equipment (UE), WiFi, CMOS, GaAs, SiGe, silicon on insulator (SOI), duplexer, filter, diplexer, multimode multiband power amplifier (MMBPA), frequency division duplex (FDD), time division duplex (TDD), carrier aggregation (CA), MIMO, digital signal processing (DSP), RF transmit (Tx), RF receive (Rx), multi-chip-module (MCM), licensed-assisted access (LAA), enhanced LAA (eLAA), adjacent channel leakage power (ACLR), internet of things (IoT), uplink (UL), downlink (DL), serial parallel interface (SPI), error vector magnitude (EVM), digital signal processing (DSP).

I. INTRODUCTION

The continuous need for high data rate in mobile applications for more users is driving the adoption of 5G long term evolution (LTE) [1-5] and WiFi 6 [6]. 5G using sub-6GHz bands and mmWave spectrum [4] together with other RF technologies such as ultra-wideband (UWB) and sensing and computation techniques [7,8] will enable multiple services, for example vehicle-to-vehicle (V2X) communications. Ultra-reliable and low latency communications (URLLC) services in mobile networks is a prerequisite for making autonomous vehicle safe together with principles and architectures used for safety-critical applications [9]. Also 5G aims to support a wide variety of new and enhanced services such as factory automation, self-driving vehicles and IoT. For some features in 5G the mobile devices as smartphones will be just a conduit for a cloud of applications. Next generation 5G smartphones need to carry over the legacy voice (2G/3G) and will also need to integrate sub-6GHz bands initially in order to provide seamless transition from 4G to 5G. There is also a lot of pressure to keep a balance between the increase functionality and the additional cost/size associated with this. Many 5G new radio (NR) requirements are specified with different requirements across bands and this is more pronounced for 5G NR due to very wide range of frequency bands. Frequency bands for 5G are divided into two frequency ranges:

- Frequency range 1 (FR1) includes all existing and new bands and corresponds to 450 MHz–6 GHz; sub-6 GHz bands.
- Frequency range 2 (FR2) includes new bands and corresponds to mmWave bands 24.25 GHz–52.6 GHz.

A typical RFFE for 5G is presented in Fig. 1 and the transition from 3G/4G FEMs to 5G FEMs poses the following challenges:

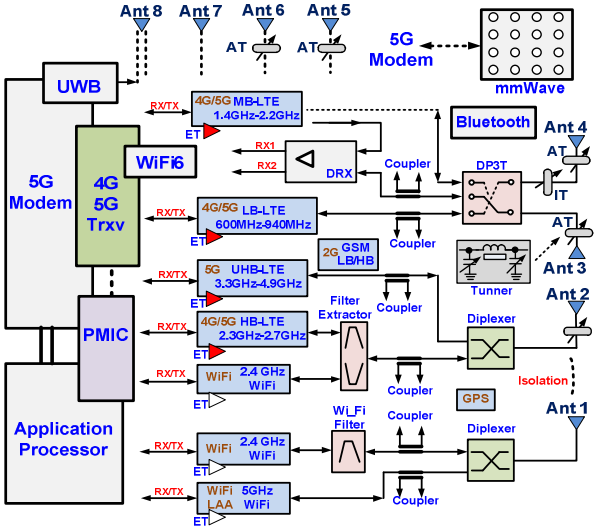

Fig. 1. 4G/5G RF front end diagram.

- Improve the power efficiency for mmWave FR2 radios; most probably FR2 will be used mainly for downlink in mobile applications [10, 11].
- Increase the number of antennas to 6-8 with the requirement to reach these antennas from different 4G/5G LTE radios which have to coexist with multiple WiFi & WiFi 6 radios, Bluetooth, GPS and UWB.
- New 5G dedicated bands for sub-6 GHz such as n77/n78 (3.3-4.2 GHz), n79 (4.4-4.5 GHz) and eLAA bands B46, B47 (5.15 GHz-5.92 GHz).
- Wider channel bandwidth up to 100MHz for FR1 where new techniques for envelope tracking (ET) are required.

978-1-7281-0586-4/19/$31.00 ©2019 IEEE

- 5G high power user equipment (HPUE) requires 26 dBm at the antenna port.
- Dual-sim operation for voice under 2G (GSM) and data (3G/4G/5G) which will increase the linearity requirements for multiple Tx/Rx paths operating at the same time.
- Higher peak to average power ratio waveforms for uplink (UL) such as 256 QAM; this requires power amplifier (PA) back-off with lower distortions, noise and less than 1.85% EVM.
- LAA and eLAA will be introduced as part of 5G as a possibility for bandwidth aggregation with a licensed anchor LTE band in UL and DL.
- Intra-coexistence with actual 3G/4G bands in 5G re-farmed bands.
- Cost effective and size for 2x2 UL-MIMO and downlink (DL) data rate coverage

The LTE power delivered at the antenna required by 3GPP standard is 23dBm. With the adoption of 5G and the resulting power losses from filters/duplexers, switches, diplexers, board and impedance/aperture tuners (IT, AT) the PA is required to deliver at least 27-28 dBm assuming less than 4-5 dB total losses. For 5G LTE user equipment (UE) there is an increase from 20 MHz to 40 MHz/60 MHz for the uplink modulation bandwidth in low/mid bands as well an increase of the output antenna power for HPUE to 26 dBm and therefore an increase in the PA output power. There is also an increase in modulation bandwidth up to 100 MHz for high/ultrahigh 5G bands such as new bands n77/n78 and n79. The goal of 5G is to reach a transmission capacity of 1Gbs. The capacity of a wireless system is determined by Shannon formula as

$$C = B_w \sum_{k=1}^{k} \log_2(1 + \frac{en * S_k}{N_x + I_k}) \qquad (1)$$

To achieve higher capacity following Eq.1 these are the techniques which are incorporated in 5G:

- increase channel bandwidth B_w; eg 100MHz LTE.
- increase spatial multiplexing level k through MIMO
- increase the transmit power; such as 26dBm (HPUE).
- decrease noise N_x and improve receive sensitivity.
- reduce in-band interference on link k, especially in multiple UL Tx such as CA and MIMO.
- higher order modulation such as 256QAM for UL
- increase signal Sk through use of ET – en factor.

II. 5G FRONT END MODULE STRUCTURE

The smartphone market is changing at an incredibly rapid pace. With the transition from 4G to 5G there is a need for the geographical coverage for more than 50 bands from 500MHz to 6GHz with few stock keeping units (SKUs). In parallel there are other radio and bands used in the same time such as UWB (6-8GHz), WiFi/WiFi6 (2.4GHz/5GHz), GPS (1.17GHz, 1.5GHz), Bluetooth (2.4GHz) and NFC (13.56KHz). Sub 3GHz bands provide primary cellular coverage and 3G/4G bands will be re-farmed to 4.5G/5G. The new 5G bands will provide the primary capacity layer with multiple MIMO. All these radios need to share common antennas without jamming the other device radios. In addition, old features such as 2G GSM have to be supported together with the new feature introduced in 5G such as LAA and eLAA that use 5GHz unlicensed band as bandwidth aggregation with a licensed LTE anchor. Usually the LTE anchor is in low band (LB) (450MHz-900MHz) due to lower propagation loss [12]. For a 15m height base-station the path loss (PL) for antenna to outdoor UE for frequency below 6GHz is determined by

$$PL_{dB} = 10\log_{10} R^4 + 21\log_{10} f + K \qquad (2)$$

PL is in general dependent of $1/R^4$ and for different propagation scenarios such as outdoor-indoor the loss is dependent of $1/f^3$. Figure 2 presents the path loss for different frequencies for a 15m base-station.

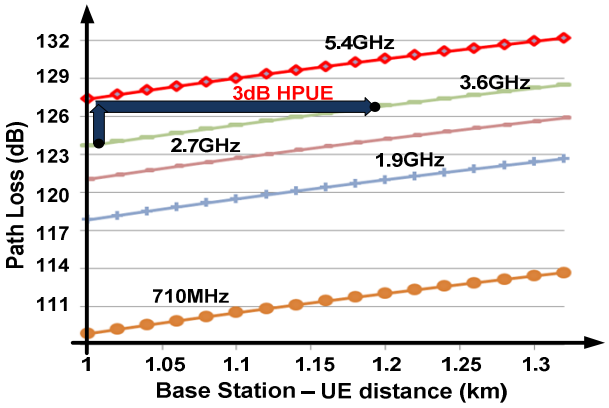

Fig. 2. Path loss versus distance and frequency.

A lot of research has been done for single die PA in different technologies such as SiGe, CMOS and SOI [13-14] and band proliferation and coexistence requirements are the biggest share and cost is determined by the acoustic filters which are placed together with SOI switches into a FEM with duplexers (FEMiD) as shown in Fig. 3. However more integration is necessary due to increase number of Rx paths for CA and MIMO also the need to integrate the LNAs and RX filters.

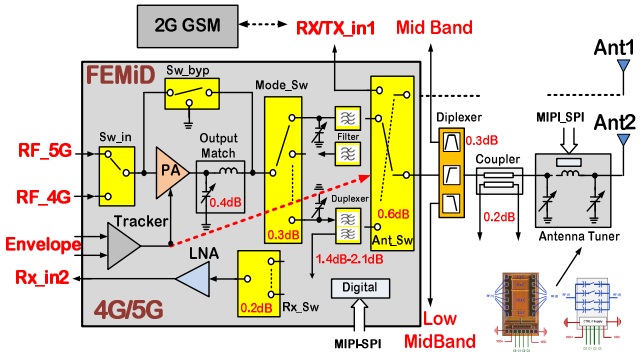

Fig. 3. LTE 4G/5G front end module typical structure.

One of the goals for 5G LTE is to reach data rates of 1GBs. The theoretical data rate (DR) is given by the formula

$$DR = n_s \bullet m \bullet (n_{cc} \bullet n_{sc} \bullet rb) \bullet n_{ss} \bullet n_{sl} \bullet ovh \bullet tdd_{ov} \quad (3)$$

where n_s represents the number of bits per symbol (8 bits for 256QAM), m represents the number of MIMO data streams, n_{cc} represents number of component carriers for carrier aggregation, n_{sb} represents number of sub-carriers, rb represents number of resource blocks, n_{ss} represents number symbols per slot, n_{sl} represents number of slots, ovh (in percentage) is the overhead required for control and coding and tdd_{ov} represents TDD duty cycle. Using this formula for 5x20MHz carrier aggregation streams, 4x4 MIMO and 256QAM the DR is

$$DR = 8 \bullet 4 \bullet (5 \bullet 12 \bullet 100) \bullet 7 \bullet 2000 \bullet 75\% \bullet 60\% = 1.2Gb/s \quad (4)$$

The same DR can be obtained using 4x4 MIMO with the new 5G MHB/UHB bands (n41, n77, n78 & n79), 100 MHz channel modulation bandwidth (BW) and 256 QAM as shown in Fig. 4 where acoustic filter multiplexers are used.

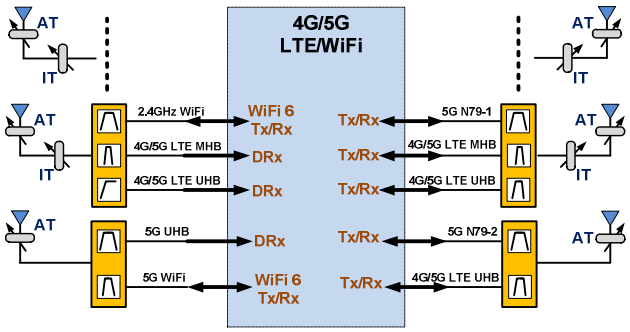

Fig. 4. WiFi and 4x4 5G MHB/UHB MIMO LTE FEM.

Usually UL/DL is asymmetric for UE in terms of data rates but to accommodate a high DL data rate still there is the need for 7-10% UL data rate for acknowledge signals. Also due to different Rx/Tx configurations between DL and UL and due to high power Tx capabilities for base-stations (40 dBm) the 4G/5G is limited in UL. This becomes more an issues for higher BW and the new 5G MHB/UHB bands. To increase the coverage 5G has adopted HPUE (Power Class 2). This will allow 19% increase in cell coverage radius (42% increases in the base-station coverage area) as shown in Fig. 2. There are two basic deployment scenarios for 4G transition to 5G networks: 5G standalone (SA) deployment and non-standalone (NSA) deployment. For NSA deployment UE should support dual connectivity (DC) for 4G LTE and 5G NR. DC will combine the coverage advantage of existing 4G LTE networks with the higher DR throughput and latency advantages of 5G NR. NSA will enable 5G NR in smartphones with a smooth evolution from 4G and will be the key to mmWave mobility as sub-6GHz anchor will be needed for roaming and handovers as shown in Fig. 5. When 4G FDD LTE and 5G NR are implemented there are challenges due to high intermodulation (IMD) distortions.

EPC: Evolved Packet Core (LTE Core Network)
NG CN: New Generation Core Network, 5G-CN
eNb: eNodeB, 4G LTE basestation
gNb: gNodeB, 5G NR basestation
UP/CP: User-Plane/Control-Plane
mmW: 5G mmW Core Network

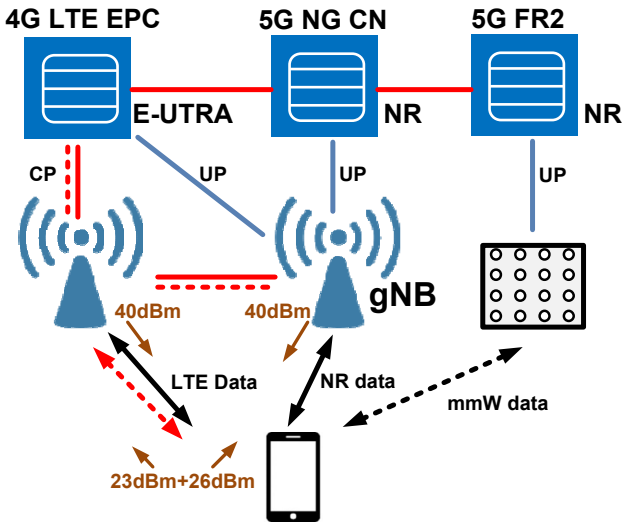

Fig. 5. 4G/5G dual connectivity (DC) configuration.

There are different ways to increase the 5G throughput such as:

- increase number of CA carriers
- enhance the coverage using lower-frequency carrier as supplementary uplink (SUL) in addition to NR's dedicated UL/DL carrier.

All these techniques such as DC and SUL have to support more than one Tx in UL together with several Rx in DL as well WiFi and other radios which will create RF interference through conductive and radiated paths. Intermodulation products are determined by all the RF Tx paths as well all other clock related activity (charge pump, SPI clocks, etc). There are few types of interference due to simultaneous UL and DL over different bans in CA configurations which will degrade the Rx sensitivity (desense):

- Interference from sub-harmonic mixing for CA case when the higher UL frequency signal is a multiple of the lower frequency (Band 7 and Band 27/CA case) and desense the low band Rx.
- Interference from the harmonic of lower frequency UL signals to the higher frequency DL when the harmonic of UL lands into UL Rx frequency band. For example when a UE is transmitting on Band 3 4G/LTE and receiving on 5G NR bands n77/n78. Second harmonic of Band 3 will land into 5G NR Rx for bands n77/n78. Another CA case for desense is when 3rd harmonic (H3) from low band lands in RX band high band as presented in Fig. 6.
- Intermodulation distortions from IMD product between different Tx frequencies and/or clock frequencies.

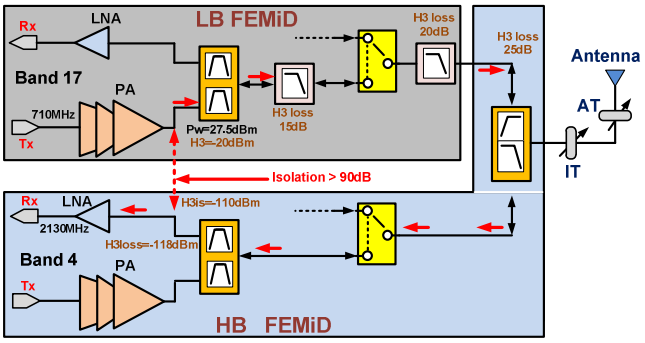

Fig. 6. Low band to high band desense due to third harmonic.

As presented in Fig. 6 to avoid any desense due to third harmonic at least 90 dB attenuation/isolation is required which is very challenging even using FEMiD shielding. From this perspective, two or more Tx might coverage highest power consumption for 5G FEM is determined by the PA. With the two or more RF transmitters operating in the same time there are higher linearity requirements for antenna SOI switches as well antenna tuning elements. For example assuming sensitivity of a typical LTE 5MHz (25RBs) as -101.5 dBm and 4.5 dB margin the linearity requirement IIP3 to avoid jamming assuming two Tx1 and Tx2 (Fig, 7) is given by

$$IIP_3 = \frac{P_{Tx2} + 2P_{Tx1} - P_{IMD}}{2} = \frac{23 + 2 * 23 - (-106)}{2} = 87.5dBm \quad (5)$$

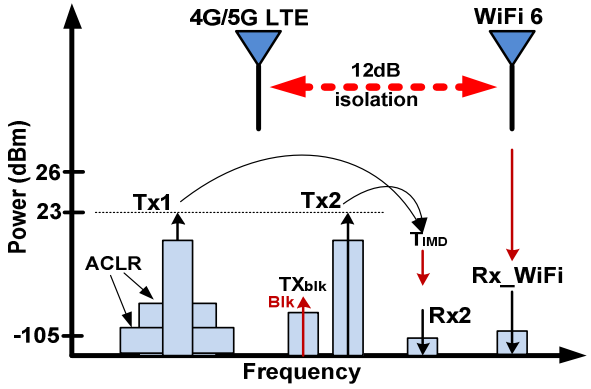

Fig. 7. Intermodulation distortions and WiFi desense.

Assuming an external blocker at -30 dBm and a Tx2 uplink signal at 23 dBm the switch linearity IIP2 is given by

$$IIP_2 = P_{blk} + P_{Tx2} - P_{IMD} = -30 + 23 - (-106) = +99dBm \quad (6)$$

In addition to WiFi coexistence with LTE bands 7, 40 and 41 single LTE due to uplink CA and limited antenna isolation might be also a desense of the WiFi . With the adoption of 5G all these desense scenarios need to be considered.

III. 4G/5G POWER AMPLIFIERS

The RF PA is one of the critical components within FEM because of efficiency and linearity requirements for 4G/5G as expressed by adjacent channel leakage power ratio (ACLR) which have to be achieved with high efficiency for all the power levels. With the adoption of 256QAM for 5G UL the PA linearity expressed through error vector magnitude (EVM) is started to be challenging to be met (less than 1.85%), although 5G will allow 4-5dB maximum power reduction (MPR). A number of techniques have been used to meet the efficiency and linearity requirements, the most extensively used and researched being Doherty and ET PAs [15, 16]. The adoption of both techniques has been possible by advances in digital signal processing (DSP) and technology scaling such as 14nm/7nm FinFET. Doherty techniques provide high efficiency but have limitation in terms of broadband operation, operation in back-off mode and load mismatch [17]. Doherty amplifiers with n-away structures to increase the bandwidth (Fig. 8) are going to be used in 5G base-station [18].

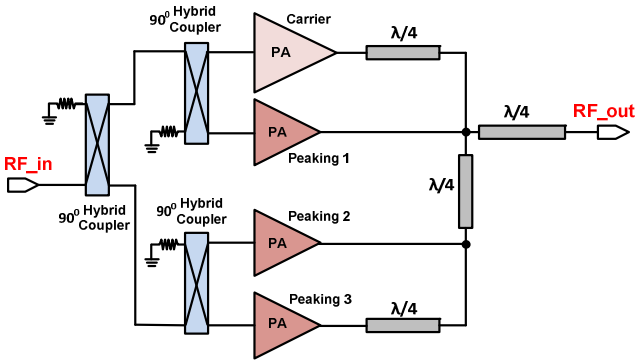

Fig. 8. 3-way Doherty amplifier structure.

In mobile applications, such as smartphones, ET is used with a broadband PA with class E output match for low, middle and high bands. The class E PA concept has been introduced in [19]. The optimum series feed inductance L and parallel capacitance C can be obtained by

$$L = 0.732\frac{R}{\omega} \quad , \quad C = \frac{0.685}{\omega R} \quad (7)$$

The technology used by PAs is mainly GaAs and the typical structure is presented in Fig. 9. The output match includes also 2fo and 3fo harmonic traps and the ET is applied to the last stage. The last stage can be also ET biased tracked to further increase the efficiency.

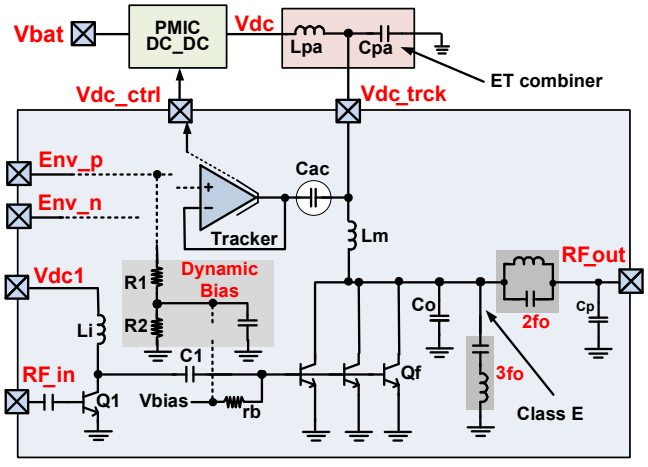

Fig. 9. ET and power amplifier with class E output match.

IV. RF SWITCH IMPLEMENTATION

The FEMiD include several SOI RF switches and a typical switch structure for one arm is presented in Fig. 10.

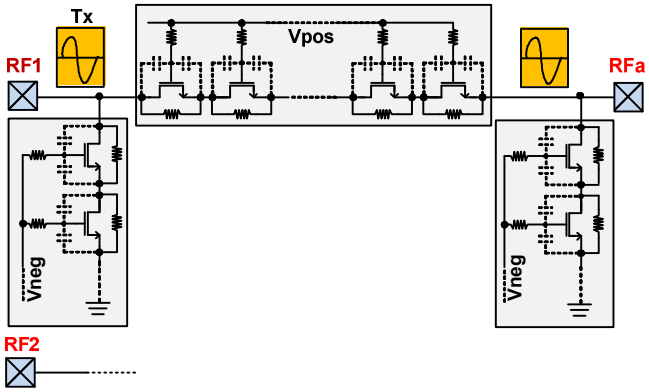

Fig. 10. SOI switch schematic.

For OFF FETs the peak RF voltage across drain-source for each transistor assuming equal voltage division is

$$\left|V_{DS\_peak}\right| = 2(V_{Th} - V_{NEG}) \tag{8}$$

The number of series FETs (n) is determined by the maximum RF power applied and the RF breakdown voltage V_{DS_peak}

$$P_{\max} = \frac{V_{Tx\,\max}^2}{2 * Z_0} = \frac{2(nV_{DS\_peak})^2}{Z_0} \tag{9}$$

The insertion loss (IL) and input intercept point (IIP3) for a series-shunt switch are defined by the equations

$$IL = 10\log\left[\left(1+\frac{Ron}{2Zo}\right)^2 + \left(\frac{2\pi Coff\,(Ron+Zo)}{2}\right)^2\right] \tag{10}$$

$$IIP\,3 = 10\,\log\left(\frac{Isat^{\,2}\,(Ron\,+2\,Zo\,)^4}{4\,RonZo^{\,2}}\right) + 30 \tag{11}$$

where *Ron* is the on-state channel resistance of the switch

$$Ron = n\frac{1}{\mu Cox\,\frac{w}{l}(Vpos - Vth)} \tag{12}$$

Vpos is the voltage applied to turn on the series switch.

V. RF FRONT END MODULE FILTERS

The advanced of the smartphones and transition from 4G to 5G with high requirements for different RF coexistence scenarios and also the manufactures demand for global phones drive the need for the use of many acoustic filters. In the early 2G/3G generations filter requirements have been handled using surface acoustic filters (SAW) but with the evolution to 4GG/5G and higher RF frequencies there is a high demand for bulk-acoustic-wave (BAW) resonators filters. SAW and BAW are complementary technologies and SAW can be manufactured and used up to around 2.5 GHz (Fig.11). BAW technology is capable to create narrow band filters up to 6-8% of the carrier frequency.

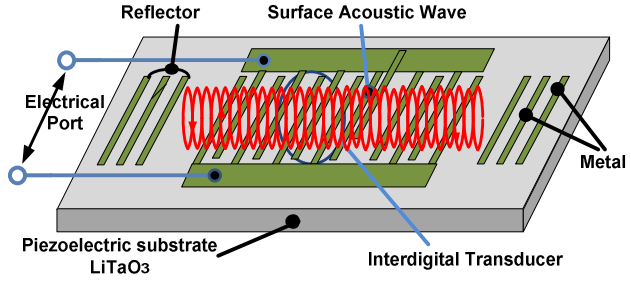

Fig. 11. SAW acoustic filter structure.

To keep the acoustic waves from dissipating into silicon substrate an acoustic Bragg reflector is created using thin layer as in solidly mounted resonator BAW (BAW-SMR). Another approach etches a cavity underneath the active area as in film bulk acoustic resonator (FBAR). Both types of BAW filters (Fig.12) present quality factors of 2,000 to 3,000 usually higher than SAW filters.

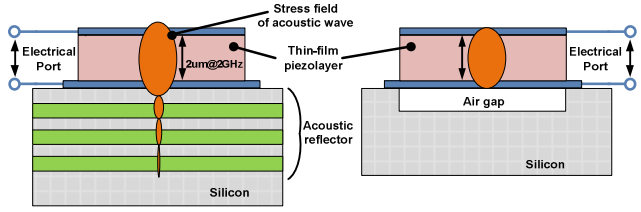

Fig. 12. BAW-SMR and FBAR filter structures.

In Fig. 13 a BAW filter characteristic used for WiFi and 5G n41 band coexistence is presented.

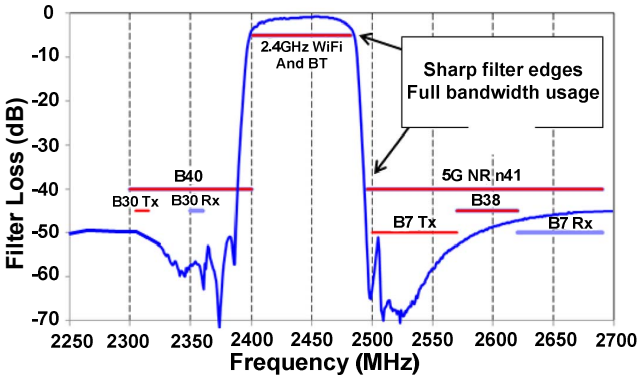

Fig. 13. WiFI BAW filter rejection.

VI. RF FRONT ANTENNA TUNERS

Actual smartphones use several antennas and based on the best impedance matching and propagation path the switching between antennas with high linearity double pole double through (DPDT) is one of the several diversity schemes. This is used to improve the quality and reliability of the RF wireless link to base-station. 5G smartphones will use 6-8 antennas which will cover several bands. For these reasons antenna tuners (AT) are used together with impedance tuners (IT) for antenna mismatch as presented in Fig. 14.

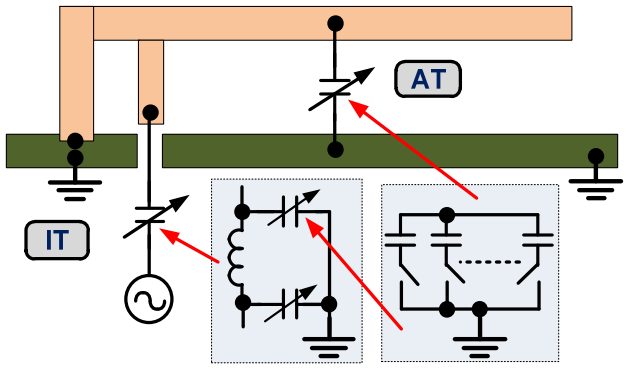

Fig. 14. Antenna and impedance tuners.

Antenna bandwidth is given by the formula

$$\frac{df}{f} = k\frac{(a/\lambda)^3}{\eta} \tag{13}$$

where a is antenna length, λ is the wavelength, η is the antenna radiation efficiency. From (13) covering wider bands can be obtained using larger antennas or lower radiation efficiency which both are undesirable and explain the need of using antenna tuners. Fig. 15 presents the antenna efficiency after tuning for a low band antenna.

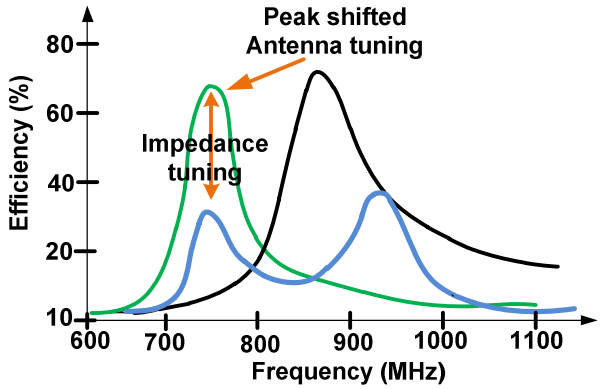

Fig. 15. Low band antenna efficiency with tunning.

VII. ENVELOPE TRACKING

ET techniques can be seen as an extension of the Shannon theory for anisotropic systems as presented in Fig. 16. In (1) the factor ***e*** represents the increase of the output signal when the envelope signal is aligned with the RF signal going into the system PA. In ET the power supply voltage delivered to a RF PA is following the envelope signal through a shaping table circuit which resides in the 4G/5G modem and therefore provides the required voltage for the PA to operate in linear region without clipping. With the migration to 5G NR where higher modulation bandwidth is required as well HPUE the location of the ET relative to the PA has an impact on the memory effects, intermodulation distortions and noise. From this perspective the ET is integrated in close proximity to the PA [14] as shown in Fig. 17 to reduce these effects which will impact the Rx noise and ACLR.

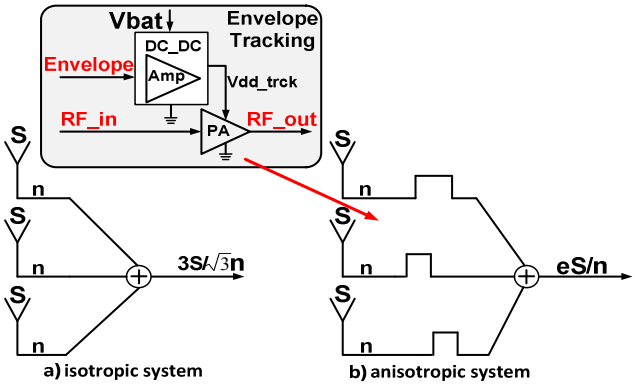

Fig. 16. a) isotropic system; b) anisotropic system

The tracker maximum frequency response *Fmax* is determined by

$$F_{\max} = \frac{SR}{2\pi V_{outpk}} \tag{14}$$

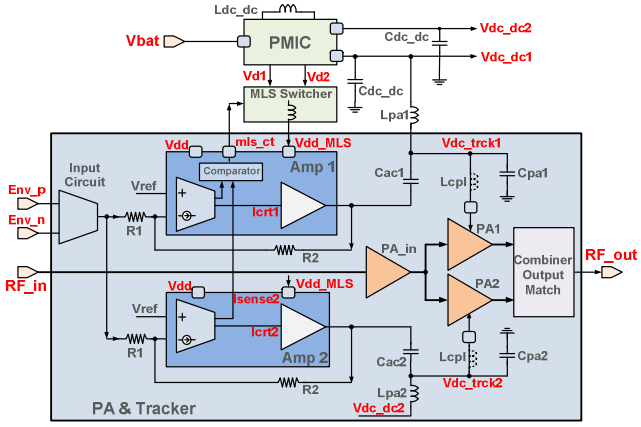

Fig. 17. 5G HPUE power amplifier and tracker structure.

where *SR* is the output slew rate of the output stage. The error amplifier structure with increased *SR* is presented in Fig. 18.

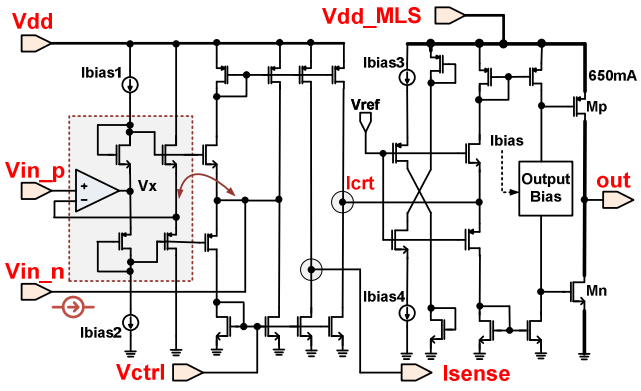

Fig. 18. ET error amplifiers Amp1 & Amp2.

If the PA is operated in ET mode *Vdd=Vdc_trck* is changing based on the envelope (instantaneous power level). The *Vdc_trck_peak* is the peak voltage and is determined by the

maximum power which has to be delivered under ET for different PAPR waveforms as expressed as

$$PAPR = 20\log(\frac{Vdc\_trck\_peak}{Vdc\_trck\_rms}) \quad (15)$$

The two error amplifiers input stages provides a current signal which control what voltage supply (*Vdd_MLS*) is applied to the output stage using a current hysteretic comparator. An increase in the output *Vdd_MLS* will increase the instantaneous *SR* for the error amplifier without delay mismatch for two paths as is the case for [20]. ET techniques can be used also to locally linearize GaN PAs for 5G mmWave as shown in Fig. 19.

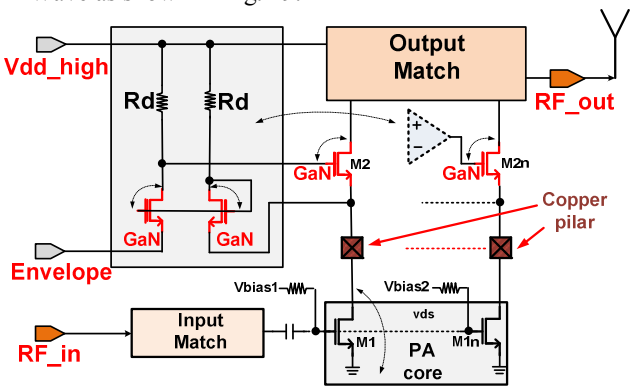

Fig. 19. ET used for GaN linearization.

The envelope signal is used to dynamical bias the top GaN cascade transistors and keep the gain transistors M1-M1n in constant gm region due to strong dependence of *gm* and *Id* in relation to *Vds*. For CMOS the relation between drain current and voltage is given by

$$I_D = \frac{1}{2}\mu C_{ox}\frac{W}{L}(V_{GS} - V_{TH})^2(1 + \lambda V_{DS}) \quad (16)$$

This presents a local ET linearization effect. Using GaN devices the technique provides enough voltage swing for high power applications such as mmWave Tx paths. This might be useful for future low feature GaN on silicon substrate.

VIII. IMPLEMENTATION AND MEASUREMENTS

The FEMs for smartphone end up in very high volume products and therefore all the cost and hardware integration associated with the functionality have to be considered and the evolution from 4G to 5G is an evolutionary process. Fig. 20 presents a photo of a MMBPA with the control circuitry and the ET amplifier on the same substrate as well a SOI switch.

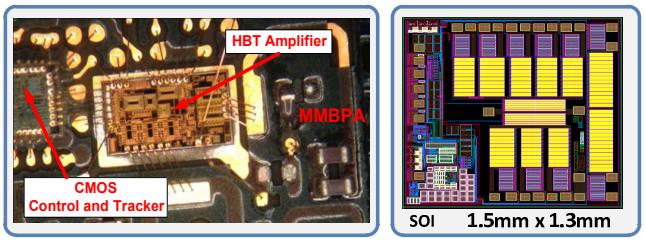

Fig. 20. MMBPA with error amplifier and SOI SP10T switch photos.

One of the RF LTE Tx characteristic is the calibration which becomes more difficult with ET, more uplink Tx bands (in 5G LTE) and more RF coexistence scenarios. Calibration requires also frequency equalization through DPD due to Tx and duplexer response for different modulation bandwidth from 1.4 MHz to 100 MHz. A method where a baseband envelope signal is aligned through a modulated RF signal and the delay is adjusted until the two baseband received signals have the same peak values is presented in Fig. 21.

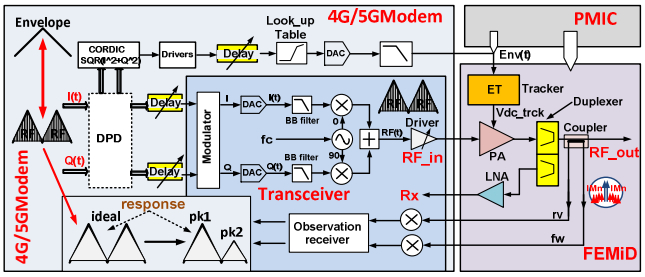

Fig. 21 FEMiD ET calibration structure.

DPD used for ET uses less modem resources and lower bandwidth for uplink Tx compared with a DPD only solution. The intermodulation distortion introduced by the delay mismatch is given by

$$IMD_{l,r} = 2\pi B_{RF}^2 \Delta_\tau^2 \quad (17)$$

where B_{RF} is the bandwidth of the RF signal and Δ_τ is the delay mismatch. The minimum between left and right intermodulation distortion determines the ACLR of the ET PA & tracker

$$ACLR = \min(IMD_{l,r}) + k \quad (18)$$

where k is a correction factor determined by PAPR and how much the PA is compressed. Figure 22 presents the ACLR value versus delay mismatch.

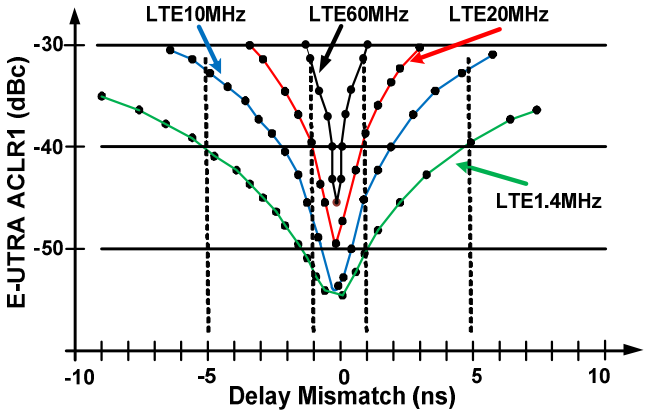

Fig. 22. ACLR versus delay mismatch.

Typically PAs use GaAs as technology and laminate substrate for matching networks due to lower losses as shown in Table I. PA and ET error amplifier are integrated into the same CMOS die using 0.18µm technology. Together with the 0.18µm SOI switches, acoustic filters and coupler are

packaged into the same MCM using advanced package solutions such as double sided BGA.

TABLE I. Output match insertion loss at 2.7GHz

Substrate Material	Insertion Loss for Band 7 – 2.5GHz
CMOS	1.3dB
High res CMOS	0.4dB
SOI	0.35dB
Laminate	0.2dB
Glass IPD	0.15dB

For 5G HPUE the PA has to deliver 30.5 dBm at the PA output to account for 4.5 dB post PA loss and 10.5 dB PAPR. This power is quite high and it's necessary to use a structure with two PAs and a combiner as presented in Fig. 16.

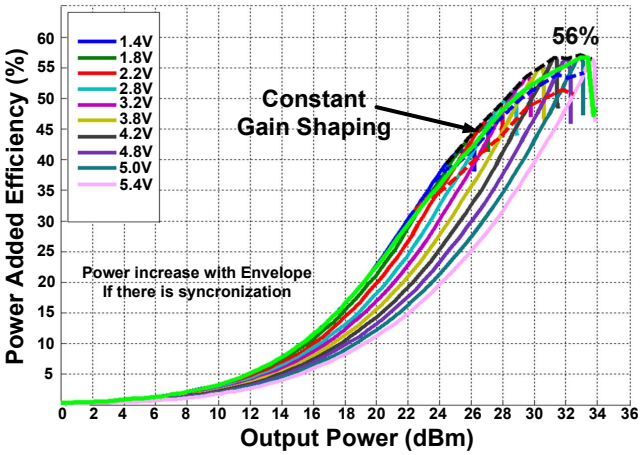

Fig. 23. Waterfall curves for 5G n77/n78 bands 3.5GHz GaAs PA.

For a FEMiD operating between 2.3 GHz to 2.7 GHz for the 4G and 5G LTE FDD/TDD new bands n7, n38, n40 and n41 the PA performance results together with the ET controller are presented in Fig. 23 and Table II.

TABLE II. Results for 2.5 GHz, LTE 80 MHz, Band n41

Pout (dBm)	Vdc_dc (V)	ACLR (dBc)	Eff (%)	RxBN@50MHz (dBm/Hz)
27	3.1	-42	33	-125
28.5	3.4	-39	36	-123
30.5	3.7	-36	38	-120
31.5	4.1	-35	39	-118

IX. CONCLUSIONS

Front end architectures for 5G have been presented with measurement details. The paper also presents an extension of Shannon theory to ET and an ET calibration method to reduce the calibration time. The novel circuits and methods will make possible the RFFE integration for next 5G smartphones.

REFERENCES

[1] A. Gupta, R. Kumar, "A Survey of 5G Network: Architecture and emerging technologies," IEEE Access, vol. 3, July 2015, pp. 1206-1232.

[2] M. Giordano, M. Polese, A. Roy, D. Castor and M. Zorzi, "ATutorial on Beam Management for 3GPP NR at mmWave Frequency," IEEE Comunications Surveys & Tutorials, vol. 21, No1, 2019, pp. 173-196.

[3] D. Pehlke, D. Brunel, K. Walsh, S. Kovacic, "Sub-6GHz 5G for UE, Optimizing cell edge user experience," IWPC 4G/5G Multi-band, Multi-Mode User Equipment, Austin, October 2017.

[4] GTI, Sub-6GHz 5G Device, White Paper, Nov. 2017.

[5] T. Rappaport, S. Sun, R. Mayzus, H. Zhao, Y. Azar, K. Wang, G.N. Wong, J.K. Schulz, M. Samimi, F. Cutierrez, "Mulllimter Wave communications for 5G cellular: It will work!," IEEE Access, vol. 1, May 2013, pp. 335-349.

[6] Wi-Fi Alliance introduces Wi-Fi 6, www.wi-fi.org, Oct. 2018.

[7] I. Dotlic, A. Connell, H. Ma, J. Clancy, M. McLaughlin, "Angle of Arrival Estimation Using Decawave DW1000 Integrated Circuits," *14th Positioning Navigation and Communications (WPNC) Workshop*, 2017, pp. 1-6.

[8] A. Al-Fuqaha, M. Guizani, M. Mohammadi, M. Aledhari, M. Ayyash, "Internet of Things; A survey on enabling technologies, and applications," IEEE Communications Survey & Tutorials, vol. 17, issue 4, 2015, pp. 2347-2376.

[9] J.H. Lala, R.E. Harper, "Architectural principles for safty-critical real-time applications," Proceedings of the IEEE, vol. 82, 1994, pp. 25-30.

[10] S. Shakib, H.C. Park, J. Dunworth, V. Aparin, K. Entesari, "A 28GHz Efficient Linear Power Amplifie in 28nm Bulk CMOS," in *2016 IEEE International Solid-State Circuits Conference (ISCC)*, Februay 2017, pp.352-354.

[11] K. Kiharoglu, M. Sayginer, T. Phelps and G.M. Rebeiz, "A 64-Element 28-GHz Phased-Array Transciver With 52dBm EIRP and 8-12Gb/s 5G Link at 300Meters Without Any Calibration," in IEEE Transactions on Microwave Theory and Techniques, vol. 66, No. 12. Dec 2018, pp. 5796-5811.

[12] 3GPP Technical Report TR 101 112 V3.2.0, "Selection procedures for the choice of radio transmission technologies of the UMTS, April 1998.

[13] D.Y.C. Lie, J. Tsay, T. Hall, T. Nukala and J. Lopez, "High-Efficiency Silicon RF Power Amplifier Design – Current Status and Future Outlook," in *IEEE international Symposium on Radio-Frequency Integration Technology (RFIT) Digest,* August 2016, pp. 1–3.

[14] F. Balteanu, "Linear Front End Module for 4G/5G LTE Advanced Applications," *2018 48th European Microwave Conference (EuMC)*, September 2018, pp. 251-254.

[15] W. H. Doherty, "A new high efficiency power amplifier for modulated waves," *Proc. Inst, Radio Eng.*, vol. 24, no. 9, pp.1163-1182, September 1936.

[16] L.R. Kahn, "Single-sideband transmission by envelope elimination and restoration," *Proc. Inst, Radio Eng.*, vol. 40, no. 7, pp. 803-806, July 1952.

[17] E. Zenteno, M. Isaksson, and P. Händel, "Output Impedance Mismatch Effects on the Linearity Performance of Digitally Predistorted Power Amplifiers," *IEEE Transactions on Microwave Theory and Techniques*, vol. 63, no. 2, pp. 754-765, Feb. 2015.

[18] J, Wong, N. Watanabe, A.V. Grebennikov, "High-power high-efficiency GaN HEMT Doherty amplifiers for base station applications," *2018 IEEE Topical Conference on RF/Microwave Power Amplifiers for Radio and Wireless Applications (PAWR)*, Jan. 2018, pp. 26-41.

[19] A.V. Grebennikov and H. Jaeger, "Class E with parralel circuit - a new challenge for high-efficiency RF and microwave power amplifiers, " in 2002 Microwave Symposium Deigest, *2002 IEEE MTT-S International Microwave Symposium Digest,* vol. 3, pp. 1627-1630.

[20] J.S. Paek, D. Kim, J.S. Bang, J. Baek, J. Choi, T. Nomiyama, J. Han, Y. Choo, Y. Youn, E. Park, S. Lee, Ik.H Kim, J. Lee, T.B. Cho, I. Kang," An 88%-Efficiency Supply Modulator Achieving 1.08μs/V Fast Transition and 100MHz Envelope-Tracking Bandwidth for 5G New Radio RF Power Amplifier,' in *2019 IEEE International Solid-State Circuits Conference (ISCC)*, February 2019, pp.238-240.